Light triggered self-construction of supramolecular organic nanowires as metallic interconnects

Vina Faramarzi, Frédéric Niess, Emilie Moulin, Mounir Maaloum, Jean-François Dayen, Jean-Baptiste Beaufrand, Silvia Zanettini, Bernard Doudin, Nicolas Giuseppone

Light triggered self-construction of supramolecular organic nanowires as metallic interconnects

Vina Faramarzi[1,2†], Frédéric Niess[1,3†], Emilie Moulin[3], Mounir Maaloum[1,3], Jean-François Dayen[1,2], Jean-Baptiste Beaufrand[1,2], Silvia Zanettini[1,2], Bernard Doudin[1,2]*, and Nicolas Giuseppone[1,3]*

[1] University of Strasbourg (UdS)

[2] DMONS Research Group – icFRC
Institut de Physique et Chimie des Matériaux de Strasbourg
CNRS-UdS – UMR 7504
23 rue du Loess, BP 43, 67034 Strasbourg cedex 2, France.

[3] SAMS Research Group – icFRC
Institut Charles Sadron
CNRS – UPR 22
23 rue du Loess, BP 84087, 67034 Strasbourg cedex 2, France.

† These authors contributed equally to this work.

* e-mails: bdoudin@unistra.fr; giuseppone@unistra.fr

The construction of soft and processable organic material that would display metallic conduction properties – i.e. with a large density of freely moving charges – represents a major challenge for electronics. Films of doped conjugated polymers are widely used as semiconductor devices, but a metallic-type transport in the bulk of such materials remains extremely scarce. Alternatively, single wall carbon nanotubes can exhibit remarkably low contact resistances with related large currents, but are intrinsically very difficult to isolate and process. Here, we report the assembly of supramolecular organic nanowires between two metallic electrodes, from a solution of triarylamine derivative, under the simultaneous action of light and electric field triggers. They display a combination of large conductivity values ($>5.10^3$ $S.m^{-1}$) and a low interface resistance ($<2.10^{-4}$ Ω.m). Moreover, the resistance of the nanowires in series with metal interfaces systematically decreases when the temperature decreases to 1.5 K, revealing an intrinsic metallic behaviour.

For more than three decades[1,2], the performances of conjugated organic polymers as active semiconducting components have been remarkably improved[3,4,5]. For instance, the intrinsic charge transport along polymer chains has been enhanced by controlled chemical or electrochemical doping[6], while crystal engineering[7,8] has reduced the incoherent inter-chain hopping regime, yielding much higher mobilities of charge carriers. Still, soft interconnects with even better conductivities and limited interface resistance values with metals are needed for low-power plastic electronics, in particular when considering the miniaturization of devices at nanoscale. In a recent and unique example, the landmark of metallic resistivity – i.e. a monotonic decrease in resistance with temperature[9] – has been reached in bulk films of doped polyaniline prepared by self-stabilized dispersion polymerisation[10]. Non mouldable metallic organic conductors have also been reported in bulk crystals made of charge-transfer salts[11], although interface resistance can possibly hinder metallic properties[12]. Indeed, the charge injection/extraction of the organic layer at the metal electrodes persists as a limiting factor owing to the contact resistance limiting devices downscaling[13,14,15,16]. Moreover, the band-type conduction regime being reduced at the metal/organic interface, the related resistance can increase exponentially as the temperature decreases, precluding a metal-like behaviour for a two-terminal device[17]. A different class of materials with metallic resistance behaviour involves a particular type of so-called metallic carbon nanotubes, which are allotropes of carbon with high aspect ratio cylindrical nanostructures (1-3 nm diameter) and a well-defined symmetry of their honeycomb crystal lattice. Optimized choice of metallic conducting electrodes material, which are quite challenging to achieve, can result in two-terminal carbon nanotubes circuits with metallic behaviour[18]. However, metallic carbon nanotubes remain intrinsically very difficult to isolate, to sort, and to position[19,20].

Soft supramolecular organic self-assemblies represent another class of emerging materials which are promising for the design of organic conductors in the 5-100 nm size range, bridging the gap between single molecules and standard thin-film organic

electronics. In particular, supramolecular self-assemblies of π-conjugated systems[21] can result in high mobility semiconductors (i.e. in which charge carriers are only scattered by a few structural defects, impurities, and phonons). Their properties are commonly tunable by the surface deposition parameters, usually through control of the solvent evaporation process[22]. These self-assemblies are structured by amphiphilic interactions, hydrogen bonds, or π-π stacking, and present a wide variety of shapes such as rod-like helical dendrimers[23], nanoribbons[24], or columnar liquid crystals[25]. For instance, the electrical conduction of π-stacked self-assembled graphitic nanotubes[26] were measured by their random deposition on Pt electrodes separated by a gap of 180 nm in length, showing a semiconductor behavior with a resistance comparable to inorganic gallium nitride (≈10 MΩ). In another example, efficient n/p-heterojunctions (in which holes and electrons can migrate in opposite directions towards electrodes) were constructed on large gold surfaces, by taking advantage of highly modified naphtalenediimides capable of ordering through supramolecular π-stacks[27]. Good mobilities were determined in these self-assemblies with short-circuit current density up to 78.10^{-6} A.cm^{-2}. However, reaching a metallic conductivity together with controlled positioning of these soft organic self-assemblies between electrodes remains an enormous challenge.

Results and discussion

Very recently[28], we described a new kind of self-assembly that is produced by the non-covalent polymerisation of catalytic amounts of triarylammonium radicals, which stack with their neutral counterparts. The process results in the formation of highly structured supramolecular triarylamine nanowires (STANWs), which aggregate into larger fibres (typically 10-50 nm in width and 50-1000 nm in length). Interestingly, in a synergistic process, STANWs permanently stabilize the charges of the initial radicals by an extended electronic delocalization within the fibres. We determine a minimal ratio of 1 charge per 160 triarylamines (but which can be higher), corresponding to an estimated

perfect delocalization length of 80±3 nm[28]. Another aspect of this process is the possibility to trigger the self-assembly by using visible light irradiation that results in the formation of a few cationic radicals and thus primes the self-assembly.

We now show how to take advantage of this triggering capability in order to probe the conductivity properties of the supramolecular assemblies by trapping them between pre-patterned metallic electrodes (Fig. 1). For that, we used a lateral device geometry with inter-electrode distance matching the observed delocalization length of STANWs in solution, i.e. in the 50-100 nm range. Large aspect ratio 'nanotrenches' of high reliability were made for this purpose, using simple optical lithography techniques (Supplementary Fig. 1)[29,30]. We fabricated trenches of typically 80±20 nm length and 100 μm width, made of Au and Ni, with leakage current below 1 pA (Supplementary Fig. 2a). We immersed this circuit in a solution of molecule **1** in 1,1,2,2-tetrachloroethane ($C_2H_2Cl_4$) (Fig. 1b), and observed current in the hundred of pA range, with related conductance well below the μS range, typically not exceeding a few nS, under a voltage difference of a few hundreds of mV (Fig. 2a,b). Subsequent sample irradiation using white light resulted in a rise of six orders of magnitude of the current, attaining values in the mA range, with the corresponding conductance values reaching several tens of mS (Fig. 2a). These two-terminal devices, with channel and interface contacts in series, exhibit a ohmic resistive nature related to high conductivity values as shown by *I*(*V)* measurements (Fig. 2c,d). We estimate a channel conductivity exceeding 5.10^3 $S.m^{-1}$, which is a minimum value supposing that the resistance originates from the bulk STANWs only. Alternatively, we estimate that interface resistance per unit length is below 2.10^{-4} Ω.m, which is a maximum limit under the hypothesis that the samples' resistance originates from interfaces only. Only single wall metallic carbon nanotubes with ballistic charge transport (i.e. exempt of charge scattering) can exhibit better values, being bound by the quantum interface resistance resulting from relaxation in the metallic terminal[18]. However it should be noted that ensembles of parallel metallic carbon nanotubes arrays exhibit optimized

conductivity of 10^4 to 10^5 $S.m^{-1}$, which is only one order of magnitude higher than our findings on STANWs[31].

After extensive rinsing of the sample with solvents, AFM imaging of the gap revealed the presence of wires similar to those observed in solution[28], with a length and positioning matching exactly the electrode gap (Fig. 1c-d), oriented along the electric field direction applied during the assembly, and with homogeneous diameters of 12±2 nm (Supplementary Fig. 3). The combination of both light-triggering and voltage-casting processes therefore results in an organic conductor geometry that fills the void between metallic contacts. We also found that applying an initial voltage threshold through the gap – concomitantly to the light irradiation – was a necessary condition for an efficient and stable formation of STANWs (Supplementary Fig. 2b). This suggests that the optimal formation scenario leading to a localised assembly starts at one electrode attracting a positively charged radical, which shares its electronic wave function with the metallic substrate, and then primes the next molecules stacking over it. The elongation process is polarized along the electric field and is self-limiting: when the other electrode is reached, its electron reservoir provides the neutralization path for stopping STANWs' growth. This scenario is also supported by the fact that a shorter exposure time to white light is able to prime the interconnect construction, with a resistance closure occurring afterwards in the dark. This process illustrates the concept of in situ self-construction which results from a light-triggered supramolecular polymerization as described in solution[28], together with an additional and precise spatial positioning. This latter and crucial aspect is brought by the perfect electric-field-casting that enforces the orientation in the device for an electrode separation around 100 nm, which corresponds to the estimated delocalization length of the self-assembly [28]. This is supported by the facts that currents measured using more distant electrodes (500 nm) increase by only 1-2 orders of magnitude compared to the immersed empty gap, and fibres fully disassemble with extensive solvent washing. We also observe a reversibility of the process when heating the connected STANWs in $C_2H_2Cl_4$ at 60 °C overnight, after which the non-covalent structure collapses and the wires

dissolve, just as happens in solution[28]. Because the radical remains stable only within the self-assembly, when breaking this later by heating above its thermal stability, the radical is subsequently reduced[32] and the system cannot self-assemble without a new light excitation / radical generation. We found no significant differences when repeating (up to six times) the self-assembly process between the electrodes, indicating that the metallic interconnects are not significantly harmed during the self-assembly and heating processes. Furthermore, after solvent drying, the structures become stable and provide reproducible results after overnight heating at 100 °C. Sample performance is not noticeably sensitive to moisture and oxygen, which constitutes a strong asset for organic electronic devices. No inert atmosphere conditions were used during the self-assembly, and samples left on the bench for one month (after AFM measurements for instance) showed reproducible transport properties.

Temperature-dependent studies revealed resistivity values systematically and reliably diminishing with decreasing temperatures, down to 1.5 K (Fig. 3a), confirming the high conductivity of our samples. We can therefore infer that the sum of ohmic contact resistance and intrinsic conductivity of STANWs has a metallic character. This also explains the contact resistance value six orders of magnitude smaller than that measured for the best conducting polymers[13,14], and four orders of magnitude lower than those of the best contacts on organic semiconductor single crystals[33]. To date, only ballistic carbon nanotubes with highly transparent resistance contacts had shown such a characteristic[18]. In addition, a similar kΩ range of resistance per fiber is estimated by counting their number through AFM imaging. We observe that perfect ohmic behavior persists up to high currents values (at atmospheric pressure (Fig. 2d), and under vacuum (Fig. 3c)). When large current stress was applied, small deviations from perfectly linear I/V curves can be attributed to sample heating (Fig. 3b). We nevertheless measure currents up to 25 mA for the lowest resistance samples submitted to a 1 V bias under vacuum conditions. The limited environmental thermalization of our suspended samples can possibly explain the measured current self-heating. This is supported by the fact that the sample slowly

recovers its initial zero bias conductance value, as expected when thermal equilibrium is retrieved in the cryostat at 4K (Supplementary Fig. 4a). In addition, another sample measured at 200K, shows similar parabolic dI/dV without hysteresis, which is attributed to the better thermal equilibrium at higher temperature environment and to the smaller voltage (current) stress value (Supplementary Fig. 4b). The corresponding current density is thus estimated in the order of 2.10^6 A.cm^{-2}, which is remarkably large for organic films and corresponds to the onset current density value for electromigration in metallic circuits. The technologically relevant value is the Blech length[34], the product of the current density by the channel's length. In our case, the estimate of 20 A.cm^{-1} is only 75 to 250 times below the so-called 'immortal interconnect' conditions[35] (i.e. with expected long term stability needed for industrial reliability).

From a mechanistic point of view, we found that the temperature-dependence data can be satisfactorily fitted using predictive models established for quasi-1D polymer metallic conduction[36] (Fig. 3a), and one may correlate these fits with the unidirectional supramolecular shape of the wires that we initially described (see previous studies)[28]. However, the hierarchical supramolecular structure of STANWs, which are made of bundles of stacked triarylamine-based fibrils, can exhibit a number of topographic defects[28], and the maximum current densities observed are still not reaching those found with ballistic carbon nanotubes (4.10^9 A.cm^{-2})[37]. The simple picture of perfect ballistic transport is therefore unlikely. If we suppose that carrier density corresponds to the density of cation radicals stabilized within supramolecular stacks, estimates based on the EPR experiments performed in solution range between 0.6% and 10%[28]. From the observed and calculated stacking geometry (see supporting information in ref. 28), the radicals density n lies in the 10^{19}-10^{20} cm^{-3} range, which typically corresponds to values encountered in semimetals, like graphite[38]. This very large density of hole carriers – for semiconductor standards – can explain the metallic character of STANWs, but this low density – for metal standards – can also explain the absence of Peierls instabilities[39] and Luttinger condensation[40] in the experimental temperature range presented here. Better

insight into structural properties of these organic interconnects are needed to unambiguously assess the dimensionality and transport mechanism in STANWs.

Owing to the spectacular nature of our findings, we took great care for discarding possible parasitic processes that might occur in our device, and we probed the hypothesis of electrode metallic residues creating shorts. We accordingly devoted a peculiar scrutiny to key control experiments, which are detailed in the supplementary information of this paper and summarized hereafter. *i*) We discarded the hypothesis of electromigration by establishing that the empty nanotrenches can withstand voltage bias much larger than those used in the self-assembly process, with or without illumination (Supplementary Fig. 5). *ii*) To probe the further involvement of an electro-migration process initiated by radical intermediate $\mathbf{1}^{\bullet+}$, we synthesized a series of analogues with electrochemical properties similar to those of STANWs building blocks, but without their propensity to self-assemble (Supplementary Table 1). In a blind test configuration, the closing of the gaps was only observed with molecules able to self-assemble, thus confirming that the conducting properties belong to STANWs themselves. *iii*) Systematic imaging of the gaps, including those which experienced several self-assembly processes, did not reveal any presence of metallic bridging structures[41,42], or extensive degradation of the metal (Supplementary Fig. 6).

Conclusions

We have discovered a fascinating soft supramolecular self-assembly which takes advantage of a self-organization process for creating metallic interconnects properties in two-point geometry. We have demonstrated that, in contrast to previous triarylamine derivatives, the self-assembly process leading to STANWs produces in turn exceptional conductivity properties. Although a theoretical understanding of such a conductivity level in STANWs remains to be explored, one may suggest that the estimated large density of hole carriers, the delocalization of the radicals throughout the triarylamine stacks[28,43,44],

and the share of their electronic wave functions with the metallic substrate[30] might be the reason explaining such a low resistance, both in the bulk and at the metal interface. The ease of solution processing, the light-triggered self-assembly, and the intrinsic self-limiting supramolecular process are shown to enable the insertion of organic interconnects in pre-determined positions by a bottom-up approach, making possible addressed control of nanoscale organic circuits. This illustrates how supramolecular self-assembly, when structured by advanced functions, will certainly represent an extraordinary tool for the next generation of smart materials. Finally, the versatile chemical structure of STANWs offers in principle numerous opportunities for tuning their electrical properties by straightforward variations using classical organic synthesis. This chemical asset might also contribute to their expected implementations towards various organic electronic devices.

Methods

Syntheses of triarylamine derivatives **1-6** (see structures in Supplementary Table 1) were performed as already described in the literature[28]. Electrodes were fabricated using edge mediated shadow mask lithography and angle deposition technique, according to a previously reported technology[29]. A Ti(5nm)/Ni(35nm)/Au(20nm) trilayer was first deposited using electron beam evaporation followed by a standard lift-off process. The second step involves a 65° angle deposition, creating a Ti(5nm)/Ni(25nm)/Au(10nm) trilayer, flowed by lift-off. The first electrode has a composition related to the superposition of the two steps, and the thinner second electrode has a composition corresponding to the second deposited trilayer, explaining the height difference observed by AFM. Nanotrenches were fabricated with a fixed inter-electrode gap of 80 nm and lengths of 100 micrometers (Supplementary Fig. 1). After checking for absence of leakage current, a solution of **1** (1mg/mL in $C_2H_2Cl_4$) was deposited by drop casting over the electrodes. A DC bias larger than 0.3 V and up to 0.8 V was immediately applied between the electrodes, and the evolution of current as a function of time was recorded using a Keitley 6517B Electrometer/High Resistance Meter. The sample was irradiated during a few seconds under a microscope condenser illumination (numerical aperture 0.55) with a 100 W halogen light source. Infrared filtering was used to limit sample heating to a few degrees, resulting in irradiation of a broadband power density of 10 $W.cm^{-2}$. The typical 10 s irradiation time corresponds to the total number of photons used in about 30 minutes for a self-assembly made in solution using a power density of ≈ 0.07 $W.cm^{-2}$, which is more than enough to trigger the self-assembly[28]. We also determined that a transition metal component in the electrode material was a necessary condition for successful interconnects self-assembly. No reliable and stable self-assembly occurred between electrodes made of Au or Pt only (with Ti adhesion layer). Self-assemblies with better than 90% success rate were obtained between Ni and Fe electrodes. We also found that covering the electrodes with Au provided better long-term sample stability, overcoming the problem of transition metals surface oxidation. In addition, performing the experiment with Au electrodes in the presence of a Ni wire dipped in the solution of **1** did not produce any conductivity/self-assembly, thus excluding a scenario where the radical would dissolve Ni(0) and generate co-self assemblies of STANWs trapping Ni

salts or even Ni wires in their core. From this series of observations, we deduce that a priming effect is provided by the transition metal substrate, likely improving the chemisorptions of triarylamine radicals by oxidation of the surface metal atoms and thus creating an optimum interface resistance. After STANWs formation, the sample was washed with chloroform, followed by extensive acetone, then ethanol washing, and finally dried with a stream of nitrogen. Low temperatures electrical measurements were carried out inside a vacuum-pumped cryostat ($P < 10^{-6}$ mbar) with 3.5 K base temperature, or in a He flow system going down to 1.5 K. Measurements of electrical properties were performed using an Agilent E5270B semiconductor parameter analyzer (DC properties), and a SRS 830 lock-in amplifier (AC properties) using a 4mV peak-to peak voltage excitation.

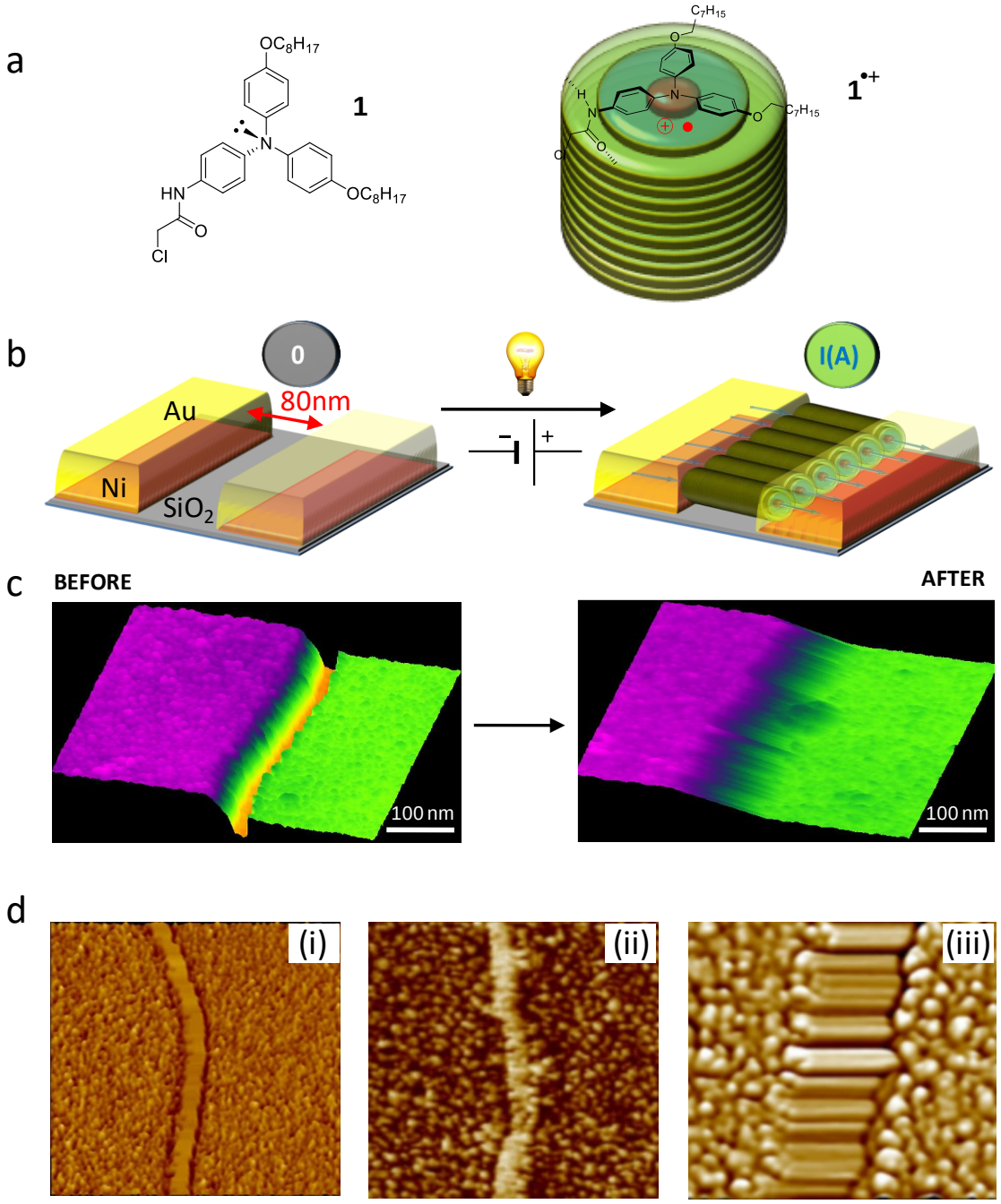

Figure 1 | Triggered self-construction process of STANWs within a nanotrench geometry together with corresponding AFM imaging. a, A solution of triarylamine **1** (1 mg.mL^{-1} in $C_2H_2Cl_4$) is drop-casted, in the dark, on nano-patterned Au/Ni electrodes schematically represented in **b** (trench width = 100 μm; length = 0.08 μm; ΔV = 0.3 - 0.8 V). The device is then submitted to a white light irradiation (Power density ≈ 10 W.cm^{-2} during 10 s), which enables the production of a catalytic quantity of radicals **1**$^{\bullet+}$. The triarylammonium **1**$^{\bullet+}$ induces a supramolecular polymerisation with neutral **1** that results in the self-assembly of STANWs aligned

in the direction of the electric field and strongly connecting the two electrodes. **c**, (*left*) Topography of the opened gap seen by AFM before light irradiation and (*right*) topography of the closed gap filled with STANWs after light irradiation. **d**, (**i**) AFM phase image of a fiber-free gap (surface scale 1500x1500 nm^2) before light irradiation; (**ii**) AFM phase image of a gap filled with STANWs (surface scale 1500x1500 nm^2) after light irradiation; and (**iii**) AFM zoom in the gap filled with STANWs after light irradiation (surface scale 250x250 nm^2).

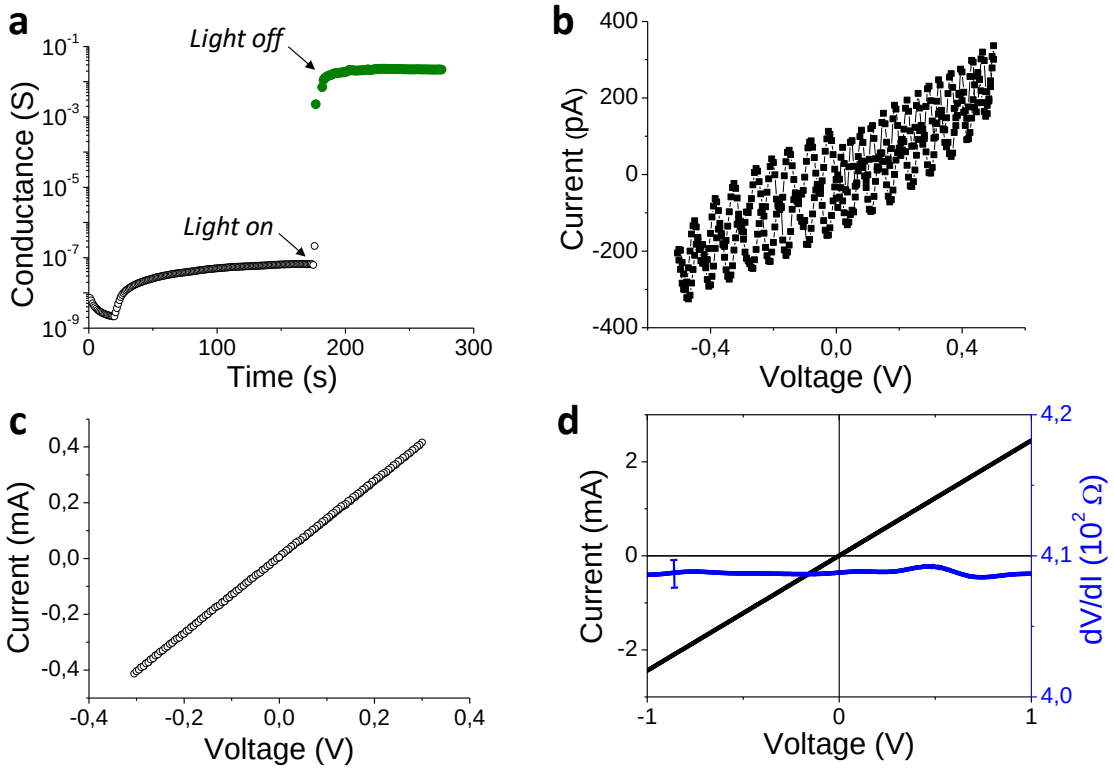

Figure 2 | Electrical properties of nanotrench devices when self-assembling STANWS. a, Conductance measured for the nanotrench device immersed in a solution of **1**, as a function of time in the dark and then (after 180 s) submitted to a white light irradiation (Power density ≈ 10 W.cm^{-2} during 10 s). The negligible initial conductance of the triarylamine derivative solution in the dark, in the 10^{-9}–10^{-7} S range, strongly increases after illumination with visible light, reaching values in the 10^{-2}–10^{-1} S range. This increase by more than 6 orders of magnitude indicates the construction of low-resistance interconnects. **b**, *I(V)* of the reference nanotrench (width = 100 μm; length = 0.08 μm) covered with a solution of triarylamine **1** (1 mg.mL^{-1} in $C_2H_2Cl_4$), and before light irradiation. The negligible residual current is attributed to ionic impurities in solution. **c**, *I(V)* measurements of the nanotrench (width = 100 μm; length = 0.08 μm) after self-assembly of **1** (1 mg.mL^{-1} in $C_2H_2Cl_4$), upon light irradiation (P=10 W.cm^{-2} during 10 s) and an initially applied voltage of 0.3 V. The two-point measurement set-up includes track resistance of typically 600-800 Ω resulting in a sample potential drop smaller than the indicated voltage scale. **d**, Current *vs* voltage curve after self-assembly, rinsing, and drying of the device. The pseudo 4 points measurement, performed at 4 K and under atmospheric pressure, shows a perfectly linear

character up to 1 Volt bias, as confirmed by the calculated differential resistance dV/dI including error bar.

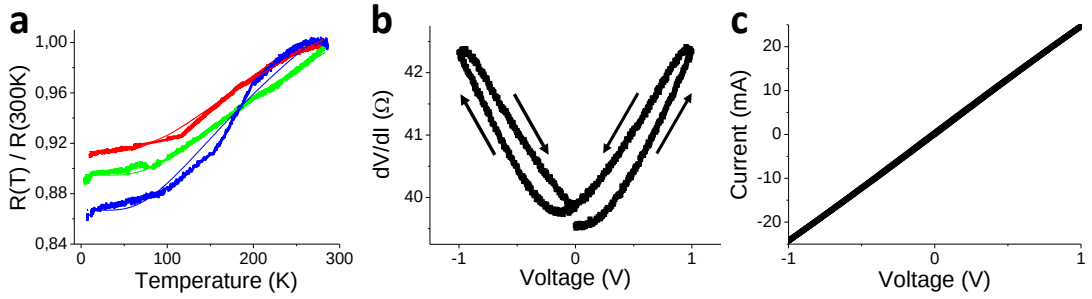

Figure 3 | Resistance of a nanotrench filled with STANWS as a function of temperature and differential conductance measured at low temperature, in vacuum, using an AC bridge technique. **a**, Normalized *R(T)* measurements of three independently prepared STANWs-functionalized devices, between room temperature and 1.5 K. The initial resistances for each sample at 300 K are the following: 22 Ω (red); 45 Ω (green); 360 Ω (blue). Each set of data is fitted (dashed lines) using a quasi 1-dimensional model of the resistance:

$$R(T) = R_0 \exp\left({}^{-\hbar\omega_0}/_{k_B T}\right) + R(T=0)$$

where k_B is the Boltzmann constant, and $\hbar\omega_0$ the energy of backscattering phonons[36]. When not indicated by an error bar, the uncertainty in the conductance measurements is smaller than the plotted line width. **b**, Increase of resistance with bias indicating possible heating of the suspended sample in vacuum, observed at 4 K. Arrows indicate the direction of voltage sweep. The hysteresis in the curve relates to the lack of thermal stability of the sample at the lowest base temperature of the cryostat. **c**, Related integrated current versus voltage curve indicating current values of several tens of mA at higher bias.

Additional Information

Supplementary information including figures and control experiments accompany this paper at www.nature.com/naturechemistry. Reprints and permission information is available online at http://npg.nature.com/reprintsandpermissions/. Correspondence and requests for materials should be addressed to B.D. or N.G.

Acknowledgments

The research leading to these results has received funding from the European Research Council under the European Community's Seventh Framework Program (FP7/2007-2013) / ERC Starting Grant agreement n°257099 (N.G.). We wish to thank the CNRS, the icFRC, and the University of Strasbourg for financial support. The support from cleanroom facilities (STnano) is gratefully acknowledged, as well as the expertise of the technical staff of the DMONS Department. This work was also partly funded by the NanoSciERA program (project INTERNET) (B.D.) and by the Agence Nationale de la Recherche: projects MOSE and SUD (B.D.), and projects Multiself and STANWs (B.D., E.M., M.M., and N.G). This work was supported by doctoral fellowships of the French Ministry of Research (V.F., F.N., S.Z., and J.-B.B.).

Author contributions

N.G. originated the work. V.F, F.N., E.M., J.-F.D., B.D., and N.G. designed the core experiment. V.F., J.-F.D., and B.D. designed the electrodes. E.M. performed the synthesis. V.F. and F.N. performed the initial key experiments, joined afterwards by J-F.D., J.-B.B., and S.Z. for completing and/or reproducing the data. M.M. performed the AFM imaging. B.D. and N.G. wrote the paper, with all authors analyzing the data, discussing, and commenting on the manuscript.

Graphical Abstract

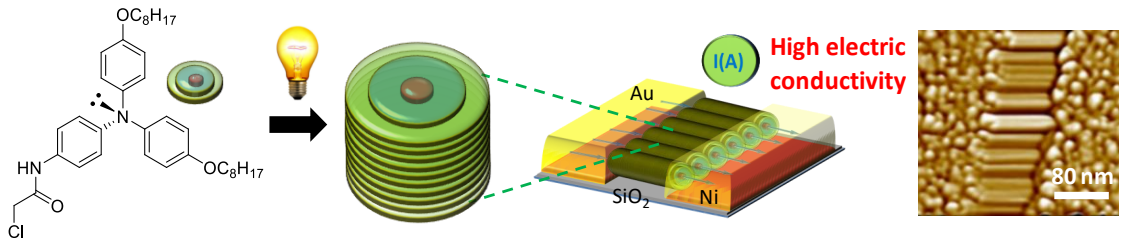

Under white light irradiation and in the presence of a voltage, solution of triarylamine derivatives have been self-assembled into organic nanowires between two electrodes. These fibers possess a very high electric conductivity as well as a metallic behaviour down to a temperature of 1.5 K.

References

1. Shirakawa, H., Louis, E.J., MacDiarmid, A.G., Chiang, C.K., & Heeger, A.J. Synthesis of electrically conducting organic polymers: Halogen Derivatives of Polyacetylene, $(CH)_x$. *J. Chem. Soc. Chem. Commun.* 578-580 (1977).
2. Heeger, A.J. Nobel lecture: Semiconducting and metallic polymers: The fourth generation of polymeric materials. *Rev. Mod. Phys.* **73**, 681-700 (2001).
3. Burroughes, J.H. *et al*. Light-emitting diodes based on conjugated polymers. *Nature* **347**, 539-541 (1990).
4. Forrest, S.R. The path to ubiquitous and low-cost organic electronic appliances on plastic. *Nature* **428**, 911-918 (2004).
5. Miller, R. D. & Chandross, E. A. Introduction: Materials for Electronics. *Chem. Rev.* **110**, 1-2 (2010).
6. Bredas, J.L. in *Handbook of conducting polymers*, vol. II. (ed. Skotheim TA), 859-913 (New York, Marcel Dekker, 1986).
7. Stutzmann, N., Friend, R.H., & Sirringhaus, H. Self-aligned, vertical-channel, polymer field-effect transistors. *Science* **299**, 1881-1884 (2003).
8. McCulloch, I. *et al.* Liquid-crystalline semiconducting polymers with high charge-carrier mobility. *Nature Mater.* **5**, 328-333 (2006).
9. Kohlman, R.S. *et al*. Limits for metallic conductivity in conducting polymers. *Phys. Rev. Lett.* **78**, 3915-3918 (1997).
10. Lee, K. *et al*. Metallic transport in polyaniline. *Nature* **441**, 65-68 (2006).
11. Jerome, D. & Schulz, H.J. Organic conductors and superconductors. *Adv. Phys*. **31**, 299-490 (1982).
12. Alves, H., Molinari, A.S., Xie, H., & Morpurgo, A.F., Metallic conduction at organic charge-transfer interfaces. *Nat. Mat.* **7**, 574-580 (2008).
13 . X.Crispin, *et al*. Characterization of the interface dipole at organic/metal interface. *J. Am. Chem. Soc.***124**, 8131-8141 (2002).
14. Ishii, H., Sugiyama, K., Ito, E., & Seki, K. Energy level alignment and interfacial electronic structures at organic/metal and organic/organic interfaces. *Adv. Mater.* **11**, 605-625 (1999).
15. Bürgi, L., Richards, T.J., Friend, R.H., & Sirringhaus, H. Close look at charge carrier injection in polymer field-effect transistors. *J. Appl. Phys.* **94**, 6129-6137 (2003).
16. Meijer, E.J. *et al*. Scaling behaviour and parasitic series resistance in disordered organic field-effect transistors. *App. Phys. Lett*. **82**, 4576-4578 (2003).
17. Hamadani, B.H., & Natelson, D. Temperature-dependant contact resistances in high-quality polymer field-effect transistors. *App. Phys. Lett*. **84**, 443-445 (2004).
18. Mann, D., Javey, A., Kong, J., Wang, Q., & Dai, H. Ballistic transport in metallic nanotubes with reliable Pd ohmic contacts. *Nanolett.* **3**, 1541-1544 (2003).
19. Harutyunyan, A.R. *et al.* Preferential growth of single-walled carbon nanotubes with metallic conductivity. *Science* **326**, 116-120 (2009).
20. Green, A.A., & Hersam, M.C. Processing and properties of highly enriched double-wall carbon nanotubes. *Nature Nano.* **4**, 64-70 (2009).
21. Hoeben, F.J.M., Jonkheijm, P., Meijer, E.W., Schenning, P.H.J. About supramolecular assemblies of π-conjugated systems. *Chem. Rev.* **105**, 1491-1546 (2005).
22. Schenning, A.P.H.J., & Meijer, E.W. Supramolecular electronics; nanowires from self-assembled π-conjugated systems. *Chem. Commun*. 3245-3258 (2005).

23. Percec, V. *et al*. Self-organization of supramolecular helical dendrimers into complex electronic materials. *Nature* **419**, 384-387 (2002).
24. Welte, L. *et al.* Highly conductive self-assembled nanoribbons of coordination polymers. *Nature Nano*. **5**, 110-115 (2009).
25. Samori, P. *et al.* Self-assembly of electron donor-acceptor dyads into ordered architectures in two and three dimensions: surface patterning and columnar "double cables". *J. Am. Chem. Soc*. **126**, 3567-3575 (2004).
26. Hill, J.P. *et al.* Self-assembled hexa-peri-hexabenzocoronene graphitic nanotube. *Science* **304**, 1481-1483 (2004).
27. Bhosale, R. *et al.* Topologically matching supramolecular n/p-heterojunction architectures. *Angew. Chem. Int. Ed*. **48,** 6461-6464 (2009).
28. Moulin, E. *et al*. The hierarchical self-assembly of charge nanocarriers: a highly cooperative process promoted by visible light. *Angew. Chem. Int. Ed.* **49**, 6974-6978 (2010).
29. Dayen, J.-F. *et al*. Nanotrench for nano and microparticle electrical interconnects. *Nanotechnology* **21**, 335303 (2010).
30. See also the section "Methods" below.
31. Tawfick, S., O'Brien, K., & Hart, A. J. Flexible high-conductivity carbon-nanotube interconnectsmade by rolling and printing. *Small* **5**, 2467–2473 (2009).
32. Fitzgerald, E.A., Wuelfing, P., Richtol, H.H. The photochemical oxidation of some aromatic amines in chloroform. *J. Phys. Chem.* **75**, 2737-2741 (1971).
33. Hulea, I.N., Russo, S., Molinari, A., & Morpurgo, A.F. Reproducible low contact resistance in rubrene single-crystal field-effect transistors with nickel electrodes. *Appl. Phys. Lett.* **88**, 113512 (2006).
34. Blech, A. Electromigration in thin films on titanium nitride. *J. Appl. Phys*. **47**, 1203-1208 (1976).
35. International technology roadmap for semiconductors, *Roadmap information on interconnects* (2009). http://www.itrs.net/Links/2009ITRS/2009Chapters_2009Tables/2009_Interconnect.pdf
36. Kilveson, S., Heeger, A.J. Intrinsic conductivity of conducting polymers. *Synth. Metals* **22**, 371-384 (1988).
37. Hong, S., Myung, S. A flexible approach to mobility. *Nat. Nano*. **2**, 207-208 (2007).
38. Kinchin, G. H. The Electrical Properties of Graphite. Proceedings of the Royal Society of London. Series A, Mathematical and Physical Sciences, **217**, 9-26 (1953).
39. Grüner, G. The dynamics of charge-density waves. *Rev. Mod. Phys*. **60**, 1129-1181 (1988).
40. Egger, R., Bachtold, A., Fuhrer, M.S., Bockrath, M., Cobden, D.H., & McEuen, P.L. Luttinger liquid behaviour in metallic carbon nanotubes, interacting electrons in nanostructures. Haug, R., & Schoeller H. Eds, *Lecture Notes in Physics* **579**, 126 (Springer 2001).
41. Lau, C.N., Stewart, D.R., Williams, R.S., & Bockrath, M. Direct observation of nanoscale switching centers in metal/molecule/metal structures. *Nanolett.* **4**, 569-572 (2004).
42. Borghetti, J. *et al.* Electrical transport and thermometry of electroformed titanium dioxide memristive switches. *J. Appl. Phys.* **106**, 124504 (2009).
43. Pal, S.K., *et al*. Resonating valence-bond ground state in a phenalenyl-based neutral radical conductor. *Science* **309**, 281-284 (2005).

44. Haddon, R.C. *et al*. Localization of spin and charge in phenalenyl-based neutral radical conductors. *J. Am. Chem. Soc*. **130**, 13683-13690 (2008).